JOURNAL OF APPLIED ELECTROCHEMISTRY **27** (1997) 1198–1206

Electrochemical characterization of Fe–Ni–P alloy electrodeposition

K. SRIDHARAN, K. SHEPPARD

Department of Materials Science and Engineering, Stevens Institute of Technology, Hoboken, NJ 07030, USA

Received 28 March 1995; revised 2 December 1996

In this study we have investigated the electrodeposition of amorphous iron–nickel–phosphorus alloys from a sulfate electrolyte. Fe–Ni alloys are known to exhibit an 'anomalous' type of plating behaviour in which deposition of the less noble metal is favoured. We have found that the codeposition of phosphorus from hypophosphite in the electrolyte led to a reversal to a 'normal' behaviour. This reversal was due both to the suppression of iron and enhancement of nickel partial currents. The overall deposition process is dominated by the hydrogen evolution reaction. This is exacerbated by the low pH needed to codeposit sufficient phosphorus to achieve an amorphous structure.

Keywords: *alloy, amorphous, anomalous, hydrogen, iron, nickel, phosphorus, plating*

1. Introduction

Electrodeposition offers the possibility of a low cost, low temperature route to producing amorphous, metallic alloy coatings or electroformed complex shapes not achievable by other metallic glass forming technologies. Although Ni–P and Ni–Fe electrodeposits have received considerable attention, little has been published on electrodeposition from the ternary iron–nickel–phosphorus system. In a previous study [1] we have shown the feasibility of producing amorphous Fe–Ni–P electrodeposits over a wide range of compositions from a mixed sulfate bath. A study to characterize electrodeposition from this system is reported here. First we examined the deposition of the binary Fe–Ni alloy and then considered the effect of incorporating phosphorus from a hypophosphite source.

1.1. *Fe–Ni alloys*

Various baths and plating conditions for depositing Ni–Fe alloys have been reported in the literature. The primary interest has been Permalloy (80Ni–20Fe) deposits for magnetic applications. Srimathi *et al.* [2] have concisely reviewed investigations in this field up to 1981. Alloy plating baths are normally prepared by mixing the sulfate or chloride salts of iron and nickel. Typical Permalloy electrolytes contain forty times as much nickel as iron in order to achieve the desired deposit composition. This amount of nickel is necessary to overcome the effects of anomalous codeposition. Anomalous codeposition is a term used by Brenner [3] to describe the preferential deposition of the less noble element during alloy plating.

Several models have been postulated to explain the anomalous deposition behaviour of the Ni–Fe system [3–7]. The model developed by Dahms and Croll [6, 7] which has gained a wide acceptance, relates the anomalous behaviour to a local pH increase at the electrode/electrolyte interface as a result of hydrogen evolution. It is postulated that the preferential precipitation of ferrous hydroxide compared to nickel hydroxide causes inhibition of nickel deposition while allowing iron discharge through the hydroxide film.

Romankiw and co-workers [8, 9] have employed a stripping voltammetry technique at a rotating ring disk electrode (RRDE) to characterize the deposition of thin Ni–Fe permalloy films. They found that agitation had little effect on the iron polarization behaviour close to the deposition potential. However, at more cathodic potentials, the iron partial current became independent of potential and depended on cathode rotation speed. Both these observations indicate that the iron deposition is under mass transport control. The nickel deposition was not affected by agitation. In the presence of iron, the polarization curves shifted to more cathodic potentials implying that nickel deposition is inhibited when iron codeposits. Dahms and Croll [6, 7] also observed that the iron polarization is shifted in the anodic direction when iron codeposits with nickel. The Dahms and Croll model was revised by Andricacos and Romankiw [9] who suggested that trace amounts of ferric ion Fe^{3+} present in the plating solution causes the precipitation of ferric hydroxide $Fe(OH)_3$. It was proposed that this film is responsible for the selective discharge of iron ions.

Grimmett *et al.* [10–12] compared d.c., pulse and pulse-reverse electrodeposition of iron–nickel alloys. For all three techniques the iron content increased initially, reached a maximum and then decreased with increasing current density. These results are similar to those reported by Andricacos and Romankiw [9] and are characteristic of anomalous codeposition. D.c. and pulse-plated alloys had similar iron contents,

0021-891X

with the iron partial currents always higher than the nickel partial currents. However, the difference decreased significantly at higher cathodic potentials. The anomalous behaviour was significantly reduced with pulse-reverse plating. The iron and nickel partial currents in pulse reverse were essentially the same. These experimental results agreed with calculations based on the Hessami–Tobias model [13] for anomalous codeposition. They suggested a steady state deposition model in which the anomalous process was controlled by the discharge rates of intermediate monohydroxide species namely $Fe(OH)^+$ and $Ni(OH)^+$ rather than by precipitation of $Fe(OH)_3$ as proposed by Romankiw [8, 9]. Grande and Talbot [14, 15] also support the monohydroxide as the controlling species during Ni–Fe deposition.

Similar investigations to determine the effects of pulsing and pulse reversal in the presence of organic additives on Ni–Fe alloys were conducted by Popov *et al.* [16]. Linear sweep voltammetry showed that when both metals were present in solution, the resulting polarization curves were not a superposition of those of iron and nickel. The effects of pulse reversal were similar to those of Grimmett *et al.* [12]. Organic additives were found to be effective in suppressing hydrogen evolution.

1.2. *Phosphorus alloys*

Amorphous metallic alloys are normally supersaturated solid solutions containing a metalloid such as phosphorus and/or boron. Electroless Ni–P was the first metallic glass to be synthesized and has been studied extensively. Although phosphorus has not been deposited alone, alloys of phosphorus with iron group metals (mainly nickel and cobalt) have been electrodeposited from aqueous baths.

Binary Ni–P amorphous alloys have been prepared both by electrodeposition as well as autocatalytic (electroless) deposition. The Ni–P electrodeposition process traces back to the pioneering work by Brenner [17]. The electrolytes typically are combinations of nickel sulfate and chloride with phosphorous and phosphoric acids. Sodium hypophosphite has also been used as a source of phosphorus. The mechanism of phosphorus codeposition is not fully understood, however an indirect reduction process has been suggested by several authors [18–20]. Brenner [3] suggested that the polarization of the inducing element aids in phosphorus codeposition. Brenner also indicated that hydrogen may act as an inducing element when it accompanies the discharge of iron-group metals.

Carabajal and White [21] have electrodeposited amorphous Ni–P alloys from a sulfate/chloride bath with phosphorous/phosphoric acids. The deposition rate of phosphorus was greater than that of nickel at low overpotentials. This trend was reversed at high overpotentials. Decreased surface H^+ ion concentration at larger overpotentials (due to hydrogen evolution) was thought to result in reduced phosphorus codeposition. An indirect mechanism was postulated as follows:

$$6\,H^+ + 6\,e^- \longrightarrow 6\,H$$

$$H_3PO_3 + 6\,H \longrightarrow PH_3 + 3\,H_2O$$

$$2\,PH_3 + 3\,Ni^{2+} \longrightarrow 3\,Ni + 2\,P + 6\,H^+$$

Phosphine gas is an intermediate product in the reduction of phosphorous acid by hydrogen. Phosphine then reacts with the nickel ions in solution to codeposit phosphorus. Observations supporting the indirect mechanism were also made by Zeller *et al.* [22] and Harris *et al.* [23].

Electrodeposits of Ni–Zn and Ni–Zn–P alloys were studied by Swathirajan *et al.* [24–26]. Potentiodynamic and galvanostatic stripping methods (similar to Romankiw *et al.* [8]) yielded partial currents for the zinc and nickel in the Ni–Zn. While the stripping regions for zinc and nickel could be clearly separated in the binary alloy, this was not possible for Ni–Zn–P because phosphorus caused a considerable surface segregation of nickel. This led to a large positive shift in the stripping potential for zinc and consequent lack of peak separation. It is for this reason that the stripping technique was not considered for our study. Swathirajan *et al.* obtained partial currents for zinc and nickel from the ternary alloy composition and Faraday's law. The partial current for phosphorus was calculated assuming a one electron reduction of the hypophosphite to elemental phosphorus based on an indirect reduction process that has been suggested by several authors [18–20, 26]:

$$Ni^{2+} + 2\,e^- \longrightarrow Ni$$

$$H_2\,PO_2^- + 2\,H^+ + e^- \longrightarrow P + 2\,H_2O$$

$$2\,H^+ + 2\,e^- \longrightarrow H_2$$

The evolution of hydrogen gas, an undesirable side reaction in electrodeposition, reduces the hypophosphite enabling codeposition of phosphorus in the alloy.

2. Experimental details

2.1. *Electrochemical characterization*

Cyclic and linear sweep voltammetry experiments were employed to electrochemically characterize the electrodeposition process. A standard three-electrode cell was used with a Pine Instruments model ASR2 rotating disc electrode (RDE). Titanium working electrodes were used since most of the alloy coatings were plated on to titanium substrates for experiments to determine the effects of the plating variables [1]. The disc electrode surface was polished on a wheel to a 0.05 μm alumina finish after each experiment. The counter electrode was a platinum mesh separated from the solution by a fritted-glass tube. A Luggin capillary probe separated the bulk solution from the saturated calomel reference microelectrode. The cell was maintained at 60 ($\pm$1) °C in a water bath.

The sulfate electrolytes used in the polarization studies were the same as those used for galvanostatic

deposition. The sulfate bath is one that has been used for nickel-phosphorus plating [27, 28] and was modified by the addition of ferrous sulfate. It should be noted that these solutions have up to an order of magnitude lower metal concentration than typical electrolytes used in nickel-iron (Permalloy) deposition but have the benefit of being dilute enough to perform polarization studies. The plating solution contained a total of 30 g dm^{-3} (≈ 0.1 M metal) of ferrous and nickel sulfates, 10 g dm^{-3} sodium acetate and 10 g dm^{-3} sodium hypophosphite. Three different electrolytes were studied by varying the iron/nickel ratios in solution. All solutions were prepared from reagent grade chemicals and deionized, organic free pure water. These are designated as A, B, and C in Table 1. Experiments with only a single metal present were also conducted. Electrolytes were deaerated with pure nitrogen gas.

An EG&G PAR model 273 potentiostat interfaced to a computer was used to sweep the potential from the open-circuit or rest potential to a cathodic potential of about 1.7 Volts vs SCE and back to the rest potential. The rest potential was measured by the null method after the working electrode had been immersed in the electrolyte for 30 min. Scan rates of 5 mV s^{-1} to 200 mV s^{-1} and rotation speeds of 1000 to 3000 rpm were employed in these experiments.

2.2. *Determination of partial currents*

The partial currents for iron, nickel, phosphorus and hydrogen were determined from alloy composition, the weight of the deposit and the electrochemical equivalent of the alloys. This approach has been used by several investigators [14, 15, 25, 26] to isolate individual metal contributions during deposition. Fe, Ni, Fe–Ni and Fe–Ni–P alloys were electrodeposited from the three different electrolytes. All deposition experiments were performed galvanostatically onto anodized titanium substrates at current densities from 30 to 100 mA cm^{-2}, with the same total charge to 1 C. The alloy compositions were determined using energy dispersive X-ray analysis (EDS). This technique was also used by Carbajal and White [21] to analyse Ni–P coatings with an average error of about 1% for each element. Composition determinations were obtained at a minimum of five points on both sides of the deposit at a magnification of 100 × in order to cover a large area. Cross-sectional analysis confirmed that compositions were consistent through the thickness. The cathodic current efficiencies for single metal and alloy plating were calculated using Faraday's law.

Table 1. Fe–Ni–P alloy baths used for electrochemical studies

	Bath composition *Fe:Ni* (*bath*)	$[Fe^{2+}]$/M	$[Ni^{2+}]$/M
Bath A	90:10	0.097	0.011
Bath B	70:30	0.075	0.034
Bath C	50:50	0.054	0.057

The partial currents of iron and nickel were calculated using the deposit composition (w), the deposition time (t), the mass of the deposit (m) and electrochemical equivalent (e):

$$i_p = m\,w/100\,et$$

The hydrogen partial current density was determined by subtracting the sum of the metal current densities from the total applied current density. Also for comparison the hydrogen current was measured in a blank experiment using preplated Fe–Ni and Fe–Ni–P surfaces in the supporting electrolyte without any metal ions.

The phosphorus partial current was calculated assuming one electron reduction of hypophosphite to elemental phosphorus [26]. This assumption was deemed valid as the amount of phosphorus formed by chemical decomposition of hypophosphite is considered negligible at temperatures below 60 °C. Higher temperatures (80 °C) are needed to initiate decomposition. No electroless decomposition was observed at the temperatures of our experiments.

3. Results and discussion

3.1. *Effect of plating parameters*

It proved possible to deposit iron–nickel–phosphorus alloys that were amorphous over a wide range of compositions as reported in detail elsewhere [1]. The major findings of that study are summarized here. The iron content of deposits plated on both planar and rotating cylinder electrodes increased with an increase in the iron content of the bath. The alloys exhibited a 'normal' alloy deposition behaviour, that is, the iron compositions were lower than those predicted from the electrolyte compositions. Therefore, in the presence of hypophosphite, anomalous deposition of iron with respect to the more noble metal nickel, did not occur in contrast to Fe–Ni alloy deposition.

The iron content of the deposits increased with increasing current density. Alloy composition was found to be dependent both on bath composition and current density. Solution pH had a marked effect on the phosphorus content of the alloys. Increase in phosphorus at lower pH was considered as evidence for an indirect reduction process for phosphorus codeposition. Control of solution pH was important because ferric hydroxide precipitates around pH 3.5 to 4 leading to dull grey deposits.

3.2. *Electrochemical characterization*

To understand electrodeposition of the ternary Fe–Ni–P alloys it was first necessary to examine the electrodeposition of the individual metals iron and nickel and as a binary alloy.

3.2.1. Cyclic polarization data. Equilibrium potentials for iron and nickel are −0.44 and −0.25 V, respec-

tively. Typical voltammograms of Fe^{2+} and Ni^{2+} separately and combined in an acetate buffer solution are shown in Fig. 1. The main features of the three voltammograms are similar. When the potential of the electrode is scanned cathodically, the cathodic current begins to increase at a potential of −700 mV for iron, −400 mV for nickel and around −500 mV for the alloy. It is seen that a large polarization is required to deposit both iron and nickel. However, the addition of nickel to an iron bath depolarizes the alloy deposition and moves the deposition potential from −700 mV to approximately −500 mV. On scan reversal a larger cathodic current is measured. The difference in current between forward and reverse scans is due to two factors: (i) increased surface area of the electrode after initial metal deposition and (ii) hydrogen evolution. The area under the anodic peak, representing stripped metal, is smaller than that of the cathodic peak in all cases, indicating that during the cathodic scan a large amount of hydrogen is also codeposited.

3.2.2. Cathodic polarization data. Quantitative analyses of the mass transport and kinetic parameters can be determined from polarization studies by varying the rotating disk speed and the bath composition. The effect of mass transport was clearly seen (not shown) in the cathodic polarization curves of iron, nickel and the alloy solutions. At fixed potentials the current densities increase with rotation speeds. For a system under mixed activation and diffusion control, the total disc current is described by the Levich equation and is made up of both the kinetic current, i_k, and the limiting current, i_l, assuming first-order kinetics with respect to concentration:

$$1/i = 1/i_k + 1/i_l$$

The mass transport current i_l can be written as $i_l = Bw^{1/2}$, where $B = 0.62\,nFACD^{2/3}v^{-1/6}$ where, F is the faradaic constant, A the area of the electrode, C the concentration of the diffusing species, v the kinematic viscosity and D the diffusion coefficient of the ionic species. A plot of i^{-1} against $w^{-1/2}$ yields a slope of B^{-1} and an intercept of i_k.

Typical Levich plots at various fixed potentials are shown in Fig. 2(a)–(c) for bath A. Similar results were also obtained for bath B and bath C. The plots for iron-only solutions (Fig. 2(a)) show fairly constant slopes in the potential region −0.7 and −1.1 V vs SCE. This indicates that the same ionic species (i.e., Fe^{2+} ion) is diffusion-limited in this region. Also the constant slopes suggest that the first order assumption is probably valid. At higher cathodic potentials the slope decreases indicating that some other species is diffusion controlled in this potential region. In the case of iron solutions at potentials more cathodic than −1.3 V, hydrogen evolution from the decomposition of water seems to be the controlling reaction.

Plots for the nickel-only solutions (Fig. 2(b)) show reasonably constant slopes in the potential region −0.5 to −0.8 V vs SCE indicating the Ni^{2+} ion to be the diffusion controlled species in this region. As with iron, at higher cathodic potentials hydrogen evolution is the controlling reaction.

The Fe–Ni alloy plots show a mixed control with iron likely being the controlling species at lower overpotential. This occurs up to about −0.8 V, followed by nickel being the diffusion controlled species in the potential range −0.85 V to about −1.1 V vs SCE. At greater cathodic potentials hydrogen evolution reaction becomes dominant. However, the individual metal plots do not match exactly with those of the alloy plots. This indicates that the interaction between iron and nickel in solution is complex and the alloy curve is not mere addition of the two metal components. It is not possible to extrapolate the alloy behaviour from those of the individual metal components. Similar inability to extrapolate the alloy behaviour from those of the individual metal components has also been reported by Ying [29, 30] in the deposition of copper–nickel alloys.

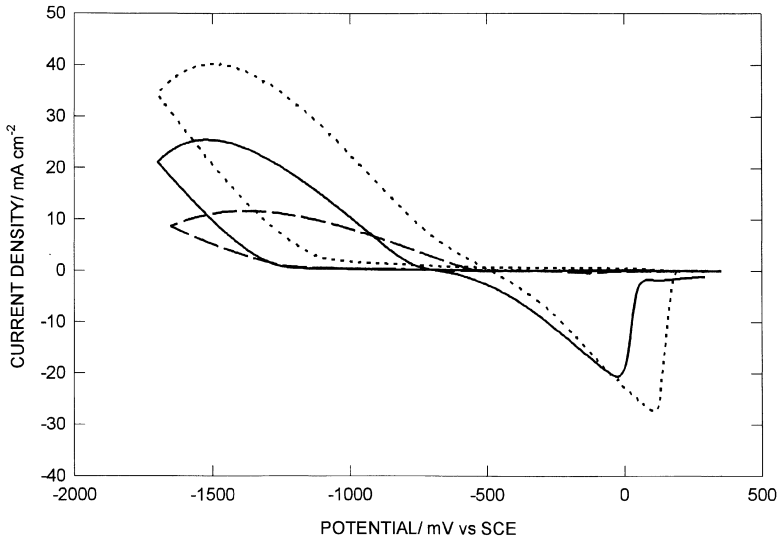

Fig. 1. Cyclic polarization curves for iron (——), nickel (— -) and iron–nickel (- - - -) solutions (bath A) at pH 2 and temperature of 60 °C.

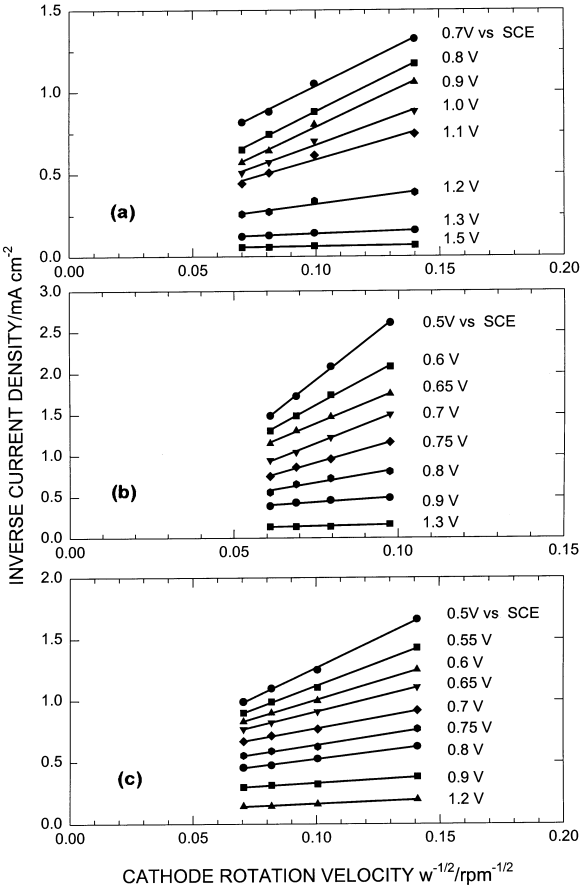

Fig. 2. Levich plots of (current density)$^{-1}$ against electrode rotation rate for (a) iron, (b) nickel and (c) iron–nickel solutions (bath A) at pH 2 and temperature of 60 °C.

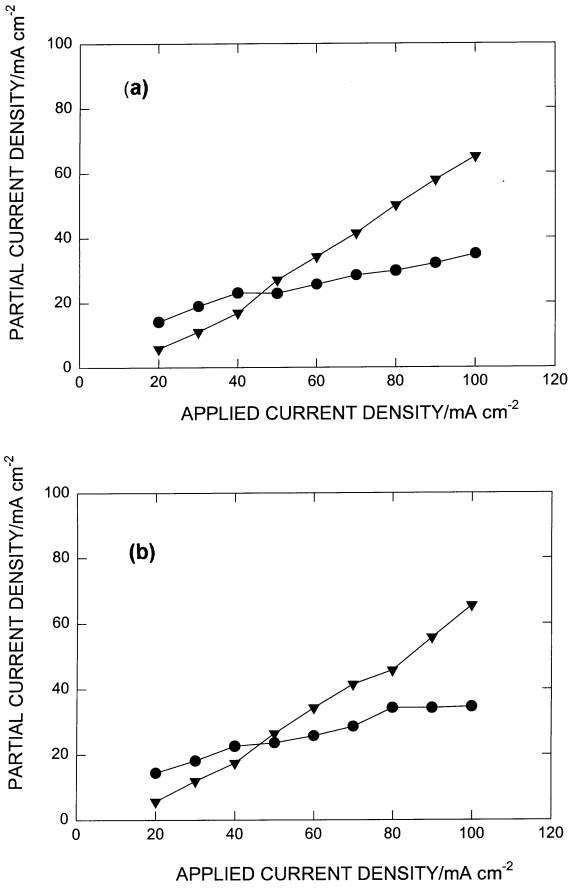

Fig. 3. Partial current densities of iron (a) or nickel (b) and hydrogen deposition from single metal baths at pH 2 and temperature of 60 °C. Key: (▼) i_{Fe} in (a), (▼) i_{Ni} in (b), (●) i_{H_2} in (a) and (b).

3.2.3. Single metal deposition. The partial current densities of single metal iron and nickel deposition from the sulfate bath at various applied current densities are shown in Fig. 3. The hydrogen partial current is determined as the difference of the metal current from the total applied current. In the range of current densities employed, namely 20–100 mA cm^{-2}, the hydrogen side reaction dominates the deposition process at low current densities up to about 50 mA cm^{-2}. Large overpotentials are required for significant iron or nickel deposition, hence the iron and nickel partial currents increase with increased applied current densities. These results are reflected in the cathodic current efficiencies shown in Fig. 4. The increase in iron and nickel partial currents results in higher cathodic efficiencies with an increase in the applied current density.

The current efficiencies for both iron and nickel deposition lie in the range 30 to 65%, indicating that almost the same amount of metal and hydrogen are codeposited in the range of current densities involved.

3.2.4. Fe–Ni alloy deposition. The effect of current density on the composition of Fe–Ni alloys electrodeposited from bath A, B and C are shown in Fig. 5. The composition of iron and nickel remain fairly constant (except for bath C) over the current density range from 30 to 100 mA cm^{-2}. The amount of iron in the deposits is more than that in the bath indicating that the deposition behaviour is anomalous, that is, the less noble iron deposits preferentially to the more noble nickel. This is true for deposition from all three electrolytes.

The extent of the deviation of the deposit composition from that of the electrolyte can be represented by the 'anomalous ratio' [25, 26].

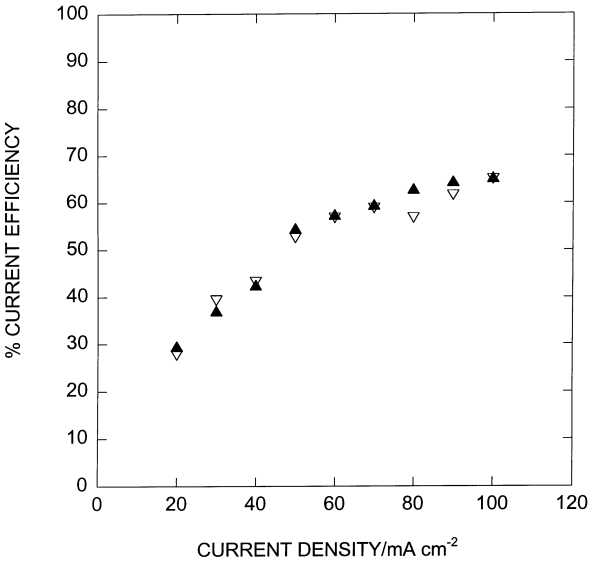

Fig. 4. Effect of current density on cathodic current efficiency of iron (▲) and nickel (▽) deposition at pH 2 and temperature of 60 °C.

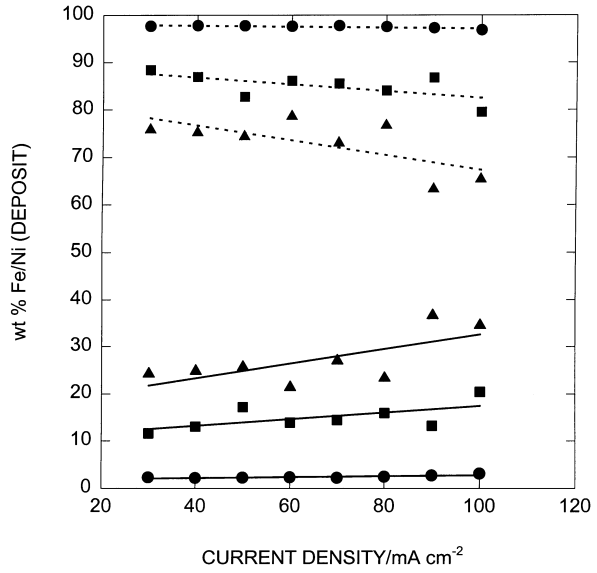

Fig. 5. Effect of current density on iron (- - - -) or nickel (——) composition in the deposit plated from different Fe–Ni baths at pH 2 and temperature of 60 °C. Key: (●) bath A, (■) bath B and (▲) bath C.

$$\text{Anomalous ratio} = \frac{\text{Molar Ratio of Fe : Ni in deposit}}{\text{Molar Ratio of Fe : Ni in electrolyte}}$$

The anomalous ratios for the three different electrolytes are shown in Fig. 6. Values of the ratio greater than one are associated with anomalous deposition. It is seen that the ratio exceeds unity over the full current density range employed in this study. The ratio begins to decrease at higher current densities (around $90-100\,\text{mA cm}^{-2}$). This corresponds to the change observed by the Levich analysis from a regime where the iron controls the kinetics (at lower current densities) to a regime of mixed control where both nickel and iron are deposited at higher current densities.

The partial current densities for iron, nickel and hydrogen codeposition from bath A and bath C are

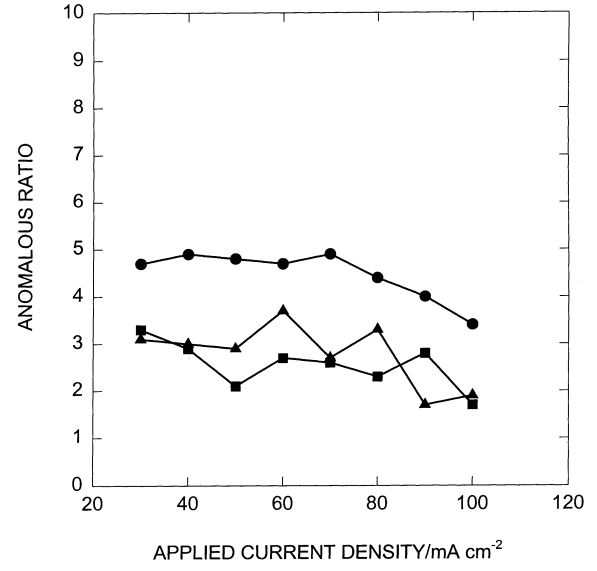

Fig. 6. Effect of the applied current density on the anomalous ratio Fe–Ni alloys deposited from different baths at pH 2 and temperature of 60 °C. Key: (●) bath A, (■) bath B and (▲) bath C.

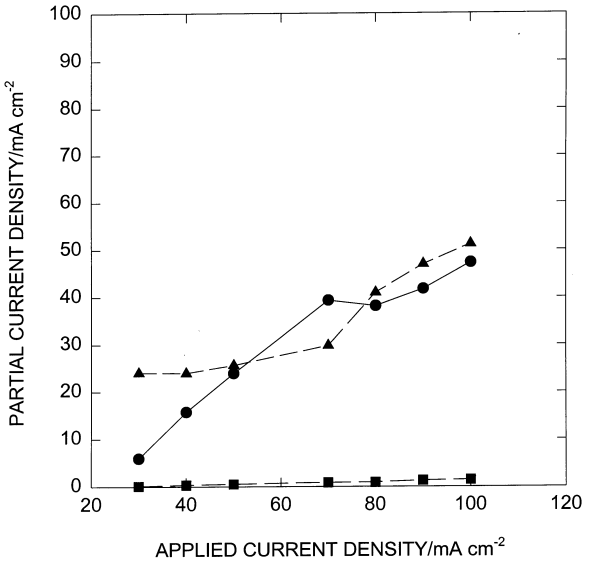

Fig. 7. Partial current densities of iron (●), nickel (■) and hydrogen (▲) deposition from Fe–Ni bath A at pH 2 and temperature of 60 °C.

shown in Figs 7 and 8. As expected from the anomalous ratios, iron carries most of the current and sufficient overpotential (i.e., higher current densities) is needed to codeposit nickel. The greater degree of supersaturation probably enhances the nucleation of nickel and therefore an increase in the nickel partial current at higher applied current densities. Unfortunately, the hydrogen evolution reaction is also accelerated at larger current densities resulting in greater hydrogen partial currents.

In the case of deposition from bath A (Fig. 7) the hydrogen side reaction is dominant only at lower current densities, at large values the hydrogen and iron currents are approximately equal. Similar results have also been reported by Podlaha *et al.* [31] for Ni–Mo alloy deposition. In contrast, deposition from bath C (Fig. 8), is dominated by hydrogen evolution at all

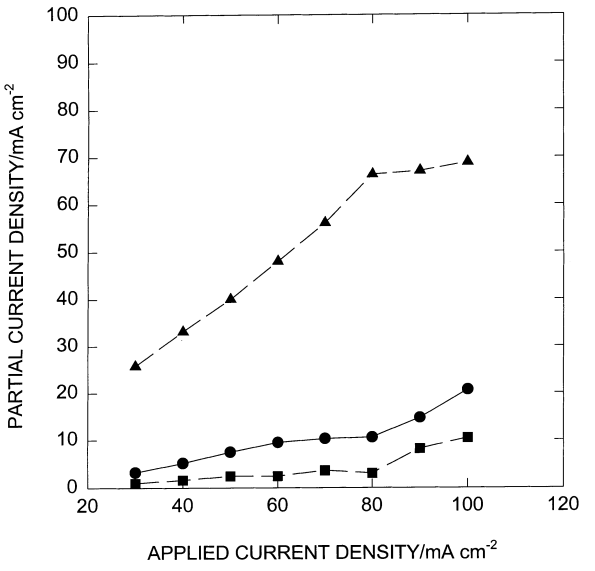

Fig. 8. Partial current densities of iron (●), nickel (■) and hydrogen (▲) deposition from Fe–Ni bath C at pH 2 and temperature of 60 °C.

current densities. The hydrogen partial current increases continuously with the applied current density resulting in lower current efficiencies for all three electrolytes. As already noted, the iron and nickel contents of deposits obtained from the three different electrolytes are each relatively uniform throughout the range of current densities.

In the case of single metal deposition, approximately the same amount of hydrogen was evolved with nickel as with iron and the hydrogen partial currents were less than those of the metal above $\approx 40\ mA\ cm^{-2}$. In contrast, the partial currents for hydrogen evolution during electrodeposition from baths B and C are significantly greater than those obtained with a single metal and greater than that from bath A. Baths B and C are richer in nickel than bath A. This is reflected in the anomalous ratio values being greater than unity. It is also consistent with the findings of others for Fe–Ni alloy deposition, that there is a strong interaction between iron and nickel that influences their partial kinetics during codeposition and also influences the hydrogen evolution reaction.

3.2.5. Fe–Ni–P alloy deposition. The effect of current density on the deposit composition is shown in Figs 9 and 10. It can be seen that the alloys exhibit a 'normal' alloy deposition behaviour, that is, anomalous ratio of less than one. This behaviour is in sharp contrast to the anomalous codeposition observed in the Fe–Ni plating.

The reversal to 'normal' alloy deposition in the presence of sodium hypophosphite could be due to suppression of the rate of discharge of iron and/or enhancement of the nickel deposition rate. Freitag *et al.* [32], in their work on nickel-rich Fe–Ni–P, report an overall reduction in the iron concentration in the presence of relatively small amounts of hypophosphite. They found that the addition of

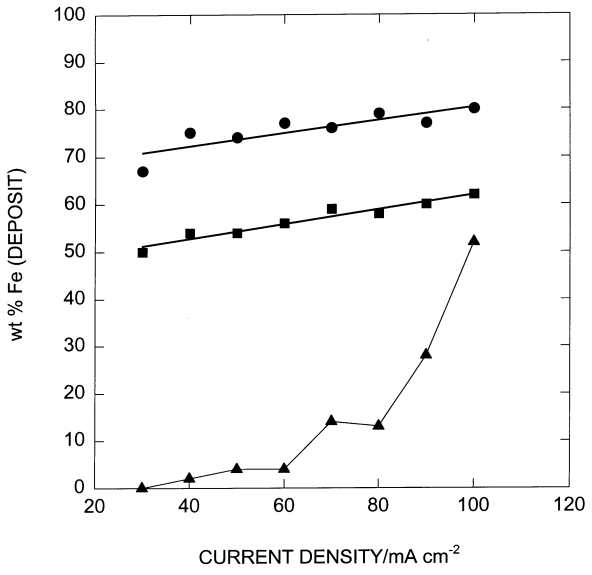

Fig. 9. Effect of current density on iron composition in the deposit plated from different Fe–Ni–P baths at pH 2 and temperature of 60 °C. Key: (●) bath A, (■) bath B and (▲) bath C.

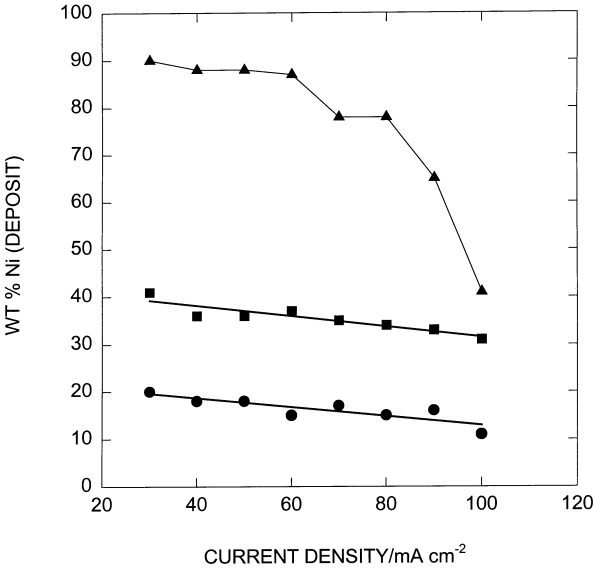

Fig. 10. Effect of current density on nickel composition in the deposit plated from different Fe–Ni–P baths at pH 2 and temperature of 60 °C. Key: (●) bath A, (■) bath B and (▲) bath C.

$1\ g\ dm^{-3}$ (we used $10\ g\ dm^{-3}$) of hypophosphite depolarized the nickel although the iron was only slightly affected.

A similar effect of hypophosphite was found in chemically (electroless) prepared Ni–Fe films by Schmeckenbecher [33]. Codeposition behaviour was found to be anomalous at a hypophosphite concentration of $5\ g\ dm^{-3}$. However, as the concentration was increased above $10\ g\ dm^{-3}$, the alloy deposition became normal. The deposition potential was also found to increase with an increase in the hypophosphite content. Our results are therefore consistent with the findings of others on the effect of hypophosphite.

For bath C the nickel contents of the deposit are greater than that in the bath. As the current density is increased (i.e., at greater polarization) the nickel content drops and approaches the electrolyte content of 50 wt%. This enhancement of nickel deposition can also be seen in the higher nickel partial currents shown in Fig. 14. A marked increase in the iron current is seen at higher current densities that moves the composition to a higher anomalous ratio. For baths A and B the effect of hypophosphite is less pronounced. Both of these electrolytes contain much more iron than nickel in solution and therefore the enhancement of nickel deposition has less impact on the composition.

In baths A and B the amount of iron in the deposits increased with an increase in current density from 30 to $100\ mA\ cm^{-2}$ as shown in Fig. 9. In the case of deposition from bath C, higher current densities were needed to codeposit iron in the alloy. This larger polarization is needed to overcome the enhancement of nickel deposition by the hypophosphite present in the electrolyte.

The increase in iron content with current density in deposits from A and B is similar to that reported by Horkans [34, 35] for Ni–Fe electrodeposition. Higher

current density is thought to cause a greater amount of iron hydroxide to precipitate at the cathode resulting in an increased amount of iron in the deposit. This process proceeds to the point where ionic diffusion through the hydroxide film limits the rate of iron deposition. The alloy composition is therefore a function of both solution composition and current density. A similar trend was reported by Bielinski *et al.* [36, 37] for Ni–Fe plating. They found, as we have, that the dependence of alloy composition is primarily due to bath composition and to a lesser degree on the current density.

The iron partial currents are less than those seen in the case of deposition without hypophosphite (Figs 11 and 13), that is, the iron deposition rate is suppressed in the presence of hypophosphite. This suppression is greater when the nickel content in the electrolyte is higher (bath C). Therefore, higher current densities are needed to codeposit any significant amounts of iron. The nickel partial currents are also greater in the presence of hypophosphite (Fig. 14). Hypophosphite therefore suppresses the deposition of iron and also promotes nickel. This effect is more pronounced when the nickel content of the electrolyte is higher.

The phosphorus contents in the deposit were found to be relatively insensitive to current density, and ranged from 7 to 12 wt% for deposition at pH 2. An increased nickel content is associated with increased phosphorus. Approximately 7 wt% phosphorus is needed to produce an amorphous deposit [38].

Hydrogen evolution dominates the overall deposition process. The hydrogen partial current increases continuously with applied current density and reaches a plateau at approximately 90 mA cm^{-2}. A similar amount of hydrogen was liberated during deposition from the three electrolytes with hypophosphite present. Without it, the hydrogen was about the same for baths B and C and lower for A.

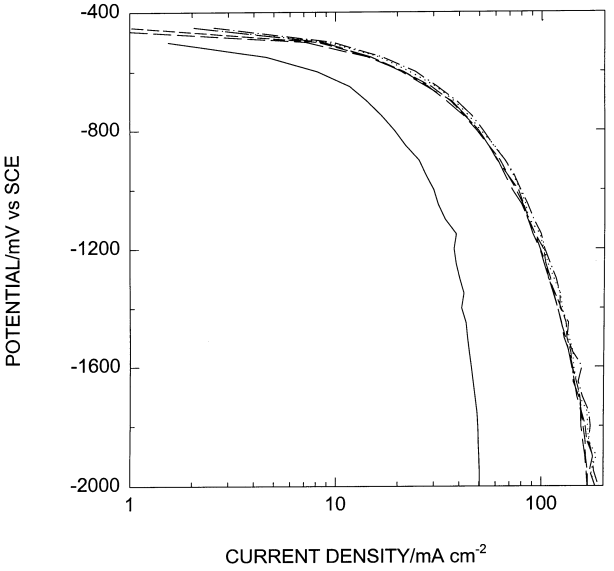

Fig. 12. Cathodic polarization of an Fe–Ni–P alloy (deposited from bath A) in an acetate buffer at pH 2 and temperature of 60 °C. Rotation rate: (——) 0, (— -) 500, (— —) 1000, (– – –) 1500, (· · · · ·) 2000 and (– · –) 2500 rpm.

The hydrogen partial current density, measured by evolving hydrogen on preplated electrodes (e.g., Fig. 12) in a solution with no metal ions, shows a limiting current of approximately 100 mA cm^{-2}. This agrees with the hydrogen partial currents determined by subtracting the metal currents from the total applied currents.

In summary the deposition of Fe–Ni–P alloys is dominated by the hydrogen evolution reaction. The hydrogen partial current increases continuously with the applied current density and reaches a plateau around 90 mA cm^{-2} and approximately the same for the three electrolytes used in this study. This domination is due to a combination of several factors. A major reason is that dilute electrolytes were used in this study. The sulfate bath we studied is one used for

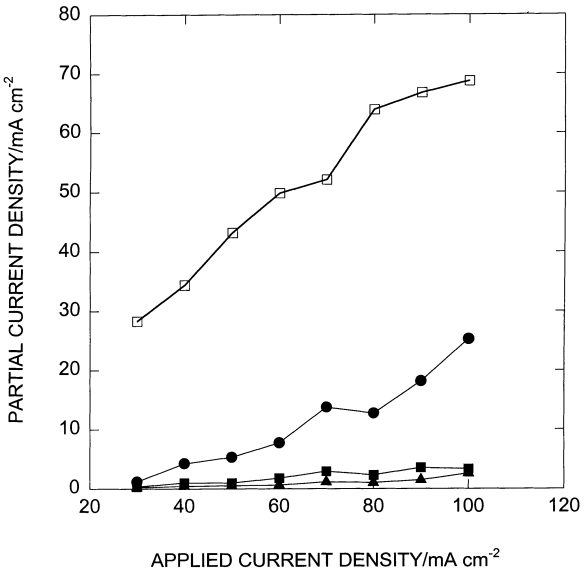

Fig. 11. Partial current densities of iron (●), nickel (■), phosphorus (▲) and hydrogen (□) deposition from Fe–Ni–P bath A at pH 2 and temperature of 60 °C.

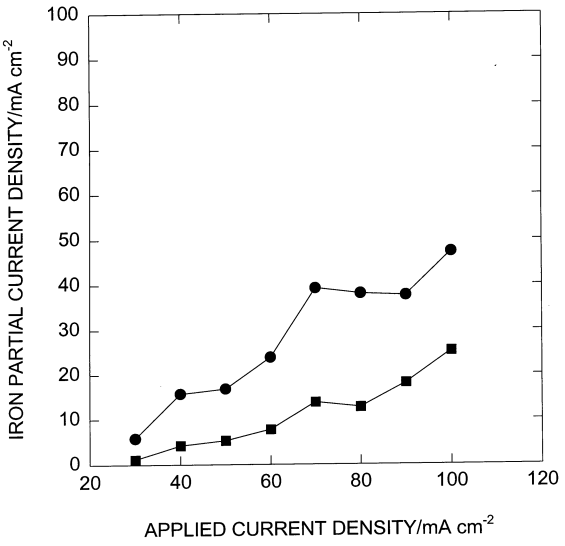

Fig. 13. Effect of sodium hypophosphite on iron partial current density for alloy deposition from bath A. Key: (●) no hypo and (■) with hypo.

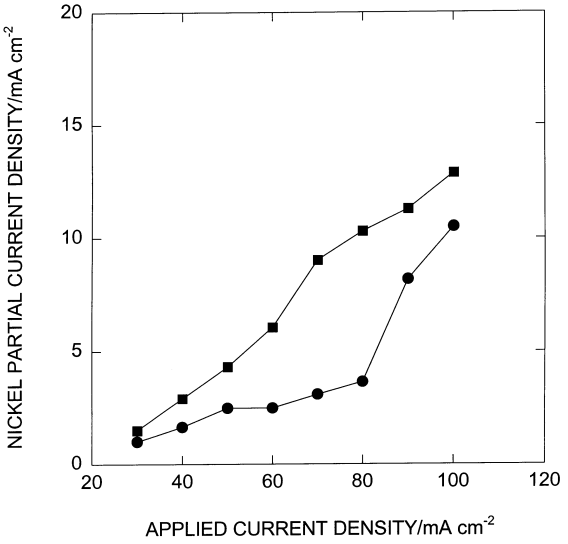

Fig. 14. Effect of sodium hypophosphite on nickel partial current density for alloy deposition from bath C. Key: (●) no hypo and (■) with hypo.

nickel–phosphorus plating and was modified by the addition of ferrous sulfate. The low metal content was attractive as a means of comparing plating and electrochemical measurements. However, the metal contents of typical Ni–Fe baths used, for example in permalloy (80Ni–20Fe), are much greater than those used in this study and this results in higher efficiencies for the latter. Secondly, no additives were used in our electrolytes in order to keep the bath as simple as possible and to eliminate adsorption/absorption effects on the electrode surface. Thirdly, electrolytes containing boric acid are typically used for Ni–Fe deposition resulting in a pH of 3. However, in our study it was necessary to use a pH of 2. This was to ensure sufficient phosphorus codeposition to obtain an amorphous structure. The lower pH enhances the evolution of hydrogen. It has been shown [16] that organic additives can be used to suppress hydrogen evolution during Fe–Ni deposition and this offers a path for applying the present knowledge to a more practical system.

4. Conclusions

(i) Fe–Ni–P electrodeposition from sulfate electrolytes exhibited 'normal' behaviour with regard to the relative compositions of the electrolyte and deposits, that is, the more noble metal deposited preferentially. This behaviour sharply contrasts the anomalous codeposition observed in Fe–Ni plating from the sulfate bath.
(ii) The 'normal' behaviour in the presence of hypophosphite in the bath was due to both suppression of the iron partial current and enhancement of the nickel partial current. It was especially marked with higher nickel content in the bath.
(iii) The low metal content of the electrolytes used in this study and the low pH needed to codeposit significant amounts of phosphorus resulted in hydrogen evolution being a dominating process.

Acknowledgements

K. Sridharan is grateful to Dr Madhav Datta of IBM, Thomas J. Watson Center, Yorktown Heights, New York for useful discussions and suggestions. Dr S.G. Fountoulakis and Bethlehem Steel Corporation are acknowledged for sponsorship of the early stages of this research.

References

[1] K. Sridharan and K. Sheppard, *Trans. Inst. Metal. Finish.* **72** (1994) 153.
[2] S. N. Srimathi, S. M. Mayanna and B. S. Sheshadri, *Surf. Technol.* **16** (1982) 272.
[3] A. Brenner, 'Electrodeposition of Alloys', 2 vols, Academic Press, New York (1963).
[4] V. V. Sysoeva and A. L. Rotinyan, *Doklady Akad. Nauk USSR* **144** (1962) 1098.
[5] A. T. Vagramyan and T. A. Fatueva, *J. Electrochem. Soc.* **110** (1963) 1030.
[6] H. Dahms and M. J. Croll, *J. Electrochem. Soc.* **112** (1965) 771.
[7] H. Dahms, *J. Electroanal. Chem.* **8** (1964) 5.
[8] P. C. Andricacos, J. Tabib and L. T. Romankiw, *J. Electrochem. Soc.* **135** (1988) 1172.
[9] P. C. Andricacos and L. T. Romankiw, *J. Electrochem. Soc.* **136** (1989) 1336.
[10] D. L. Grimmett, M. Schwartz and K. Nobe, *Plat. Surf. Finish.* **75** (1988) 94.
[11] D. L. Grimmett, M. Schwartz and K. Nobe, *J. Electrochem. Soc.* **137** (1990) 3414.
[12] D. L. Grimmett, M. Schwartz and K. Nobe, *ibid.* **140** (1993) 973.
[13] S. Hessami and C. W. Tobias, *ibid.* **136** (1989) 3611.
[14] W. C. Grande and J. B. Talbot, *ibid.* **140** (1993) 669.
[15] W. C. Grande and J. B. Talbot, *ibid.* **140** (1993) 675.
[16] B. N. Popov, K. Yin and R. E. White, *ibid.* **140** (1993) 1321.
[17] A. Brenner and G. E. Riddell, *J. Res. Nat. Bur. Stand.* **39** (1947) 385.
[18] M. Bandler and D. Z. Schellenberg, *Z. Anorg. Allg. Chem.* **340** (1965) 113.
[19] P. K. Ng, T. E. Mitchell, I. E. Locci and A. A. Ruiz, *J. Mater. Res.* **4** (1989) 300.
[20] M. Ratzker, D. S. Lashmore and K. W. Pratt, *Plat. Surf. Finish.* **73** (1986) 74.
[21] J. L. Carbajal and R. E. White, *J. Electrochem. Soc.* **135** (1988) 2952.
[22] R. L. Zeller and U. Landau, *ibid.* **139** (1992) 3464.
[23] T. M. Harris and Q. C. Dong, *ibid* **140** (1993) 81.
[24] S. Swathirajan, *J. Electroanal. Chem. Interf. Electrochem.* **221** (1987) 211.
[25] S. Swathirajan, *J. Electrochem. Soc.* **133** (1986) 671.
[26] S. Swathirajan and Y. M. Mikhail, *ibid.* **136** (1989) 374.
[27] F. Ogburn and C. E. Johnson, *Plating* **60** (1973) 1043.
[28] C. C. Nee and R. Weil, *Surf. Technol.* **25** (1985) 7.
[29] R. Y. Ying, *J. Electrochem. Soc.* **135** (1988) 2957.
[30] *Idem, ibid.* **135** (1988) 2964.
[31] E. J. Podlaha, M. Matlosz and D. Landolt, *ibid.* **140** (1993) L149.
[32] W. O. Freitag, J. S. Mathias and G. DiGuilio, *ibid.* **111** (1964) 35.
[33] A. F. Schmeckenbecher, *ibid.* **113** (1966) 778.
[34] J. Horkans, *ibid.* **126** (1979) 1861.
[35] J. Horkans, *ibid.* **128** (1981) 45.
[36] J. Bielinski and J. Przyluski, *Surf. Technol.* **9** (1979) 53.
[37] *Idem, ibid.* **9** (1979) 65.
[38] K. Sridharan and K. Sheppard, to be published in *J. Mater. Process. Technol.*